and activating ERK proteins. A heterozygous missense mutation in *MAP2K1* is known to be causal for CFCS or NS [Allanson and Roberts, 2011; Rauen, 2012]. To date, all published *MAP2K1* mutations occurred in exons 2, 3, and 6.

In this report, we present a patient clinically diagnosed with NSML, who had a de novo novel and heterozygous *MAP2K1* variant with probable pathogenicity.

CLINICAL REPORT

The patient, a 13-year-old Japanese boy, was the second child of a healthy 30-year-old mother and a healthy 35-year-old nonconsanguineous father. His two brothers were healthy. He was born by normal vaginal delivery at 41 weeks and 4 days of gestation after an uncomplicated pregnancy. His birth weight was 4,350 g (+3.2 SD), length was 51 cm (+1.0 SD), and OFC was 37 cm (+2.6 SD). He showed hypotonia and sucked poorly in the neonatal period. He raised his head at age 3 months, rolled over at 4 months, and sat unsupported at 7 months. He showed no distinctive facial features and only a few lentigines in infancy (Fig. 1A, B).

His growth was impaired with a weight of 8.25 kg (−2.1 SD), height of 76.9 cm (−1.6 SD), and OFC of 45.6 cm (−1.4 SD) at age 1 7/12 years. His weight was 11 kg (−2.5 SD), height was 90.0 cm (−2.4 SD), and OFC was 49 cm (−0.4 SD) at age 2 10/12 years. Lentigines increased on the face and the limbs (Fig. 1C, D). He walked unassisted at age 3 3/12 years, and spoke a two-word sentence at 3 years. His intellectual quotient was 60 at 4 years, and 82 at 7 years. He showed growth acceleration from age 8.5 years, accompanied by a change in voice, and was diagnosed as precocious puberty at 9 years with an advanced bone age of 11.5 years. At age 10 years, his weight was 22.1 kg (−1.5 SD), height was 130 cm (−1.2 SD), and OFC was 51.8 cm (−1.0 SD). He underwent surgical elongation of his hamstrings, which reduced the limitation of bilateral knee extension from −60° degrees to −20° degrees.

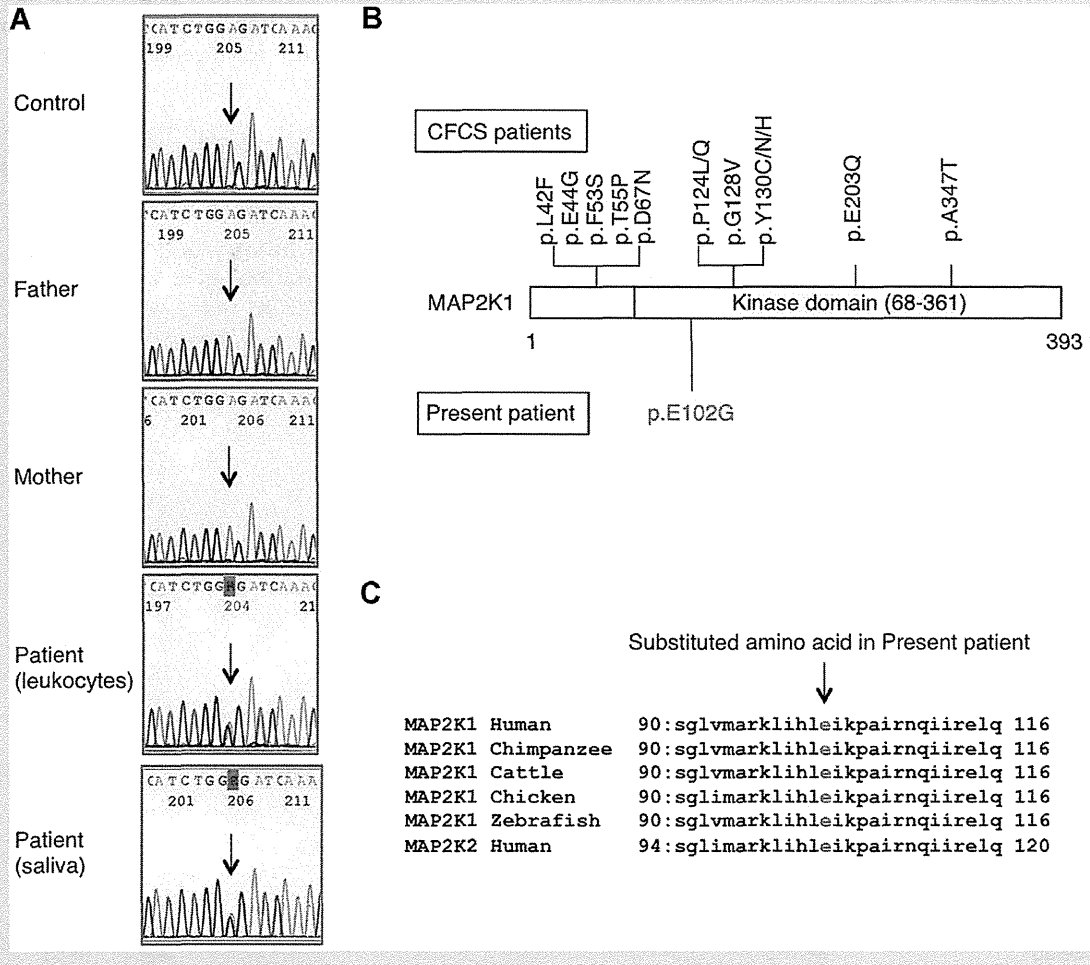

FIG. 2. A: Sanger sequencing of *MAP2K1*, showing an A→G substitution (c.305A > G, p.E102G) in exon 3, which was detected in the patient's DNA from leukocytes and saliva, but not detected in parental samples. B: MAP2K1 domain structure and location of residues altered in the present patient and previously reported patients with cardio-facio-cutaneous syndrome (CFCS). C: MAP2K1 amino acid alignment around the residue where the present amino acid change occurred. This residue is evolutionally conserved.

At age 11 years, his facial features included ocular hypertelorism, a long philtrum, thick upper and lower lip vermilions, and thickened ear helices (Fig. 1E, F). He had hyperextensible and dark skin with multiple lentigines all over the body, several café-au-lait spots, and fine wrinkles on the palms (Fig. 1G–J). He had a slender habitus with pectus carinatum, mild scoliosis, slender extremities, and limited extension of both elbows and knees (Fig. 1K). His weight was 23.0 kg (−1.8 SD) and height was 141 cm (−0.4 SD).

He had no abnormalities in the external genitalia. Resting or 24-hour ECG detected no conduction abnormalities. Echocardiography showed no congenital heart defects, pulmonary valve stenosis, or hypertrophic cardiomyopathy (HCM). Brain magnetic resonance imaging showed no structural abnormalities. He had bilateral mild sensorineural hearing loss with the threshold of 40 dB at approximately 2 kHz. G-banded chromosomes were normal.

MOLECULAR INVESTIGATION

Genomic DNA was isolated from the patient's leukocytes and saliva and his parents' leukocytes after appropriate informed consent. All coding exons and flanking introns in *PTPN11*, *KRAS*, *HRAS*, and *SOS1*, exons 6 and 11–16 in *BRAF*, exons 7, 14, and 17 in *RAF1*, exons 2 and 3 in *MAP2K1/2*, and exon 1 in *SHOC2* were amplified by polymerase chain reaction (PCR) with primers based on GenBank sequences. The primer sequences are available on request. PCR amplification was performed under standard condition using Taq DNA polymerase. After amplification, the PCR products were gel-purified and sequenced on the ABI 3500xL automated DNA sequencer (Applied Biosystems, Carlsbad, CA). A heterozygous missense variant (c.305A > G, p.E102G) was identified in exon 3 of *MAP2K1* in the patient's DNA extracted from his leukocytes and saliva. The variant was not detected in the parental samples (Fig. 2A). No mutation, other than c.305A > G in *MAP2K1*, was identified by the analysis using custom HaloPlex panel (Agilent Technologies, Santa Clara, CA) designed to identify mutations in exons and exon-intron boundaries of the following RASopathy-related genes: *PTPN11*, *HRAS*, *KRAS*, *NRAS*, *BRAF*, *RAF1*, *MAP2K1/2*, *SOS1*, *SHOC2*, *CBL*, *RIT1*, *NF1*, *SPRED1*, and *RRAS*.

DISCUSSION

The present patient had multiple lentigines, café-au-lait spots, ocular hypertelorism, growth impairment, sensorineural hearing loss, hypotonia, low average intelligence, and skeletal abnormalities.

TABLE I. Clinical Features of the Present Patient, Patients With Noonan Syndrome With Multiple Lentigines (NSML), and Patients With Cardio-Facio-Cutaneous Syndrome (CFCS) Caused by *MAP2K1* or *MAP2K2* Mutations

	Present patient	Patients with NSML [Gelb and Tartaglia, 2010]	Patients with CFCS caused by *MAP2K1* or *MAP2K2* mutations [Dentici et al., 2009]	
Causative gene	*MAP2K1*	*PTPN11* (90%) *RAF1* (n = 2) *BRAF* (n = 2)	*MAP2K1* (n = 41)	*MAP2K2* (n = 20)
Sex	Male	Male > Female	Male:Female = 9:14	
Nevi/lentigines	+	<100%	11/34 (32%)	
Café-au-lait spots	+	70–80%	5/30 (17%)	
Congenital heart defects	−	85%	25/39 (64%)	
HCM	−	70%	14/42 (33%)	
ECG abnormalities	−	23%	2/28 (7%)	
Pulmonary valve stenosis	−	25%	17/42 (40%)	
Polyhydramnios	−		20/32 (63%)	
Fetal macrosomia	+		13/25 (52%)	
Short stature	+	<50%	30/38 (79%)	
Macrocephaly	+		26/34 (76%)	
Hypertelorism	+		23/30 (77%)	
Thickened helix	+		27/30 (90%)	
Sparse hair	−		33/49 (67%)	
Sparse eyebrow	−		35/38 (92%)	
Palpebral ptosis	−		18/27 (67%)	
Flat nasal bridge	−		10/12 (83%)	
Joint limitation	+			
Failure to thrive	+		29/35 (83%)	
Intellectual disability	−	30%	43/46 (93%)	
Development delay	+		43/45 (96%)	
Hypotonia	+		40/45 (89%)	
Sensorineural hearing loss	+	<20%		
Seizures	−		16/44 (36%)	

CFCS, cardio-facio-cutaneous syndrome; ECG, electrocardiograph; HCM, hypertrophic cardiomyopathy , NSML, Noonan syndrome with multiple lentigines.

He lacked ECG conduction abnormalities, pulmonary stenosis, or abnormal genitalia. These findings were compatible with the standard diagnosis of NSML by Voron et al. [1976]. The variant c.305A > G, p.E102G was found de novo and not detected in db SNP Release 137 (http://www.ncbi.nlm.nih.gov/projects/SNP/), the Exome Sequencing Project (NHLBI-ESP) database (ESP6500SI-V2) (http://evs.gs.washington.edu/EVS/), the 1000 Genomes Project (1KGP) (http://www.1000genomes.org/), or the Human Gene Mutation Database (http://www.hgmd.cf.ac.uk/ac/index.php). In the COSMIC database, c.302_307delTGGAGA, resulting in an in-frame deletion (p.E102_I103delEI), has been identified in two samples with malignant melanoma and lung cancer (http://cancer.sanger.ac.uk/cancergenome/projects/cosmic/). The glutamine residue at codon 102 is located in the kinase domain (residues 68–361) of *MAP2A1* (Fig. 2B) and is conserved in higher organisms (Fig. 2C). Polymorphism Phenotyping v2 (PolyPhen-2) (http://genetics.bwh.harvard.edu/pph2/) predicts the variant to be possibly damaging, with a score of 0.711. In view of this evidence, the variant p.E102G may be causal for various clinical features consistent with NSML in the patient. However, no functional characterization of the variant was available and Sorting Intolerant From Tolerant (SIFT) (http://sift.jcvi.org) predicts the variant to be tolerated, with a score of 0.09.

We reviewed clinical features of the present patient, previously reported patients with NSML caused by *PTPN11* mutations in most (including two caused by *RAF1* mutations and two caused by *BRAF* mutations), and patients with CFCS caused by *MAP2K1* or *MAP2K2* mutations (Table I) [Pandit et al., 2007; Dentici et al., 2009; Koudova et al., 2009; Sarkozy et al., 2009]. Patients with NSML frequently had congenital heart defects and/or HCM, and sometimes had pulmonary valve stenosis and/or ECG abnormalities [Wakabayashi et al., 2011; Martínez-Quintana and Rodríguez-González, 2012], none of which were found in the present patient. Both patients with NSML caused by *RAF1* mutations had HCM, additionally, one had pulmonary valve stenosis, and the other had a mitral valve anomaly [Pandit et al., 2007]. One of the two patients with NSML caused by *BRAF* mutations had tetralogy of Fallot and the other had mitral and aortic valve dysplasia [Koudova et al., 2009; Sarkozy et al., 2009]. Patients with CFCS caused by *MAP2K1* or *MAP2K2* mutations frequently had congenital heart defects, polyhydramnios, characteristic facial "coarseness" (sparse hair/eyebrows, palpebral ptosis, and flat nasal bridge), and intellectual disability [Dentici et al., 2009], which were not found in the present patient. They rarely or sometimes had nevi, café-au-lait spots, or sensorineural hearing loss [Dentici et al., 2009], which were found in the present patient. Fetal macrosomia, postnatal failure to thrive/growth impairment, macrocephaly, hypotonia, developmental delay, and facial features including hypertelorism and thickened helices were shared by the present patient and over half of the patients with CFCS caused by *MAP2K1* or *MAP2K2* mutations.

In conclusion, the present patient may be the first to fit the standard clinical diagnostic criteria for NSML by Voron et al. [1976]; associated with a *MAP2K1* mutation. He lacked congenital heart defects or HCM, frequently observed in those with NSML, mostly caused by *PTPN11* mutations. He had fetal macrosomia, postnatal failure to thrive/growth impairment, macrocephaly, hypotonia, developmental delay, and hypertelorism but lacked congenital heart defect, characteristic facial features, or intellectual disability; which are frequently observed features in CFCS caused by *MAP2K1* or *MAP2K2* mutations. These observations could offer new insight into the phenotypic spectrum of RASopathies.

ACKNOWLEDGMENTS

We thank the patient and his parents for participating in this study. This work was supported by Research on Intractable Diseases from Ministry of Health, Labour and Welfare, Japan (Y.M., K.T.) and Nagano Children's Hospital Research Foundation (E.N.).

REFERENCES

Allanson JE, Roberts AE. 2011. Noonan syndrome. In: Pagon RA, Adam MP, Bird TD, et al., editors. GeneReviews® [Internet]. Seattle (WA): University of Washington; 1993–2014. Available from: http://www.ncbi.nlm.nih.gov/books/NBK1116/. Accessed March 16, 2014. .

Aoki Y, Matsubara Y. 2013. Ras/MAPK syndromes and childhood hemato-oncological diseases. Int J Hematology 97:30–36.

Dentici ML, Sarkozy A, Pantaleoni F, Carta C, Lepri F, Ferese R, Cordeddu V, Martinelli S, Briuglia S, Digilio MC, Zampino G, Tartaglia M, Dallapiccola B. 2009. Spectrum of MEK1 and MEK2 gene mutations in cardio-facio-cutaneous syndrome and genetype-phenotype correlations. Eur J Hum Genet 17:733–740.

Gelb BD, Tartaglia M. 2010. LEOPARD syndrome. In: Pagon RA, Adam MP, Bird TD, et al., editors. GeneReviews® [Internet]. Seattle (WA): University of Washington; 1993–2014. Available from: http://www.ncbi.nlm.nih.gov/books/NBK1116/. Accessed March 16, 2014. .

Koudova M, Seemanova E, Zenker M. 2009. Novel BRAF mutation in a patient with LEOPARD syndrome and normal intelligence. Eur J Med Genet. 52:337–340.

Martínez-Quintana E, Rodríguez-González F. 2012. LEOPARD syndrome: Clinical features and gene mutations. Mol Syndromol 3:145–157.

Pandit B, Sarkozy A, Pennacchio LA, Carta C, Oishi K, Martinelli S, Pogna EA, Schackwitz W, Ustaszewska A, Landstrom A, Bos JM, Ommen SR, Esposito G, Lepri F, Faul C, Mundel P, López Siguero JP, Tenconi R, Selicorni A, Rossi C, Mazzanti L, Torrente I, Marino B, Digilio MC, Zampino G, Ackerman MJ, Dallapiccola B, Tartaglia M, Gelb BD. 2007. Gain-of-function RAF1 mutations cause Noonan and LEOPARD syndromes with hypertrophic cardiomyopathy. Nat Genet 39:1007–1012.

Rauen KA. 2012. Cardiofaciocutaneous syndrome. In: Pagon RA, Adam MP, Bird TD, et al., editors. GeneReviews® [Internet]. Seattle (WA): University of Washington; 1993–2014. Available from: http://www.ncbi.nlm.nih.gov/books/NBK1116/. Accessed March 16, 2014. .

Sarkozy A, Digilio MC, Dallapiccola B. 2008. Leopard syndrome. Orphanet J Rare Dis 3:13.

Sarkozy A, Carta C, Moretti S, Zampino G, Digilio MC, Pantaleoni F, Scioletti AP, Esposito G, Cordeddu V, Lepri F, Petrangeli V, Dentici ML, Mancini GM, Selicorni A, Rossi C, Mazzanti L, Marino B, Ferrero GB, Silengo MC, Memo L, Stanzial F, Faravelli F, Stuppia L, Puxeddu E, Gelb BD, Dallapiccola B, Tartaglia M. 2009. Germline BRAF mutations in Noonan, LEOPARD, and cardiofaciocutaneous syndromes: Molecular diversity and associated phenotypic spectrum. Hum Mutat 30:695–702.

Voron DA, Hatfield HH, Kalkhoff RK. 1976. Multiple lentigines syndrome. Case report and review of the literature. Am J Med 60:447–456.

Wakabayashi Y, Yamazaki K, Narumi Y, Fuseya S, Horigome M, Wakui K, Fukushima Y, Matsubara Y, Aoki Y, Kosho T. 2011. Implantable cardioverter defibrillator for progressive hypertrophic cardiomyopathy in a patient with LEOPARD syndrome and a novel PTPN11 mutation Gln510His. Am J Med Genet A 155A:2529–2533.

Hum. Reprod. Advance Access published January 20, 2015
Human Reproduction, Vol.0, No.0 pp. 1–8, 2015
doi:10.1093/humrep/deu364

human reproduction ORIGINAL ARTICLE *Andrology*

Molecular basis of non-syndromic hypospadias: systematic mutation screening and genome-wide copy-number analysis of 62 patients

M. Kon[1,2], E. Suzuki[1], V.C. Dung[3], Y. Hasegawa[4], T. Mitsui[2], K. Muroya[5], K. Ueoka[6], N. Igarashi[7], K. Nagasaki[8], Y. Oto[9], T. Hamajima[10], K. Yoshino[11], M. Igarashi[1], Y. Kato-Fukui[1], K. Nakabayashi[12], K. Hayashi[12], K. Hata[12], Y. Matsubara[13], K. Moriya[2], T. Ogata[1,14], K. Nonomura[2], and M. Fukami[1,*]

[1]Department of Molecular Endocrinology, National Research Institute for Child Health and Development, Tokyo 157-8535, Japan [2]Department of Renal and Genitourinary Surgery, Hokkaido University Graduate School of Medicine, Sapporo 060-8638, Japan [3]Department of Endocrinology, The Vietnam National Hospital of Pediatrics, Hanoi, Vietnam [4]Department of Endocrinology and Metabolism, Tokyo Metropolitan Children's Medical Center, Tokyo 183-8561, Japan [5]Department of Endocrinology and Metabolism, Kanagawa Children's Medical Center, Yokohama 232-0066, Japan [6]Division of Urology, National Center for Child Health and Development, Tokyo 157-8535, Japan [7]Department of Pediatrics, Toyama Prefectural Central Hospital, Toyama 930-0975, Japan [8]Department of Pediatrics, Niigata University School of Medicine, Niigata 951-8510, Japan [9]Department of Pediatrics, Dokkyo Medical University Koshigaya Hospital, Koshigaya 343-0845, Japan [10]Division of Endocrinology and Metabolism, Aichi Children's Health and Medical Center, Obu 474-8710, Japan [11]Department of Urology, Aichi Children's Health and Medical Center, Obu 474-8710, Japan [12]Maternal-Fetal Biology, National Research Institute for Child Health and Development, Tokyo 157-8535, Japan [13]National Research Institute for Child Health and Development, Tokyo 157-8535, Japan [14]Department of Pediatrics, Hamamatsu University School of Medicine, Hamamatsu 431-3192, Japan

*Correspondence address. E-mail: fukami-m@ncchd.go.jp

Submitted on October 1, 2014; resubmitted on December 16, 2014; accepted on December 30, 2014

STUDY QUESTION: What percentage of cases with non-syndromic hypospadias can be ascribed to mutations in known causative/candidate/susceptibility genes or submicroscopic copy-number variations (CNVs) in the genome?

SUMMARY ANSWER: Monogenic and digenic mutations in known causative genes and cryptic CNVs account for >10% of cases with non-syndromic hypospadias. While known susceptibility polymorphisms appear to play a minor role in the development of this condition, further studies are required to validate this observation.

WHAT IS KNOWN ALREADY: Fifteen causative, three candidate, and 14 susceptible genes, and a few submicroscopic CNVs have been implicated in non-syndromic hypospadias.

STUDY DESIGN, SIZE, DURATION: Systematic mutation screening and genome-wide copy-number analysis of 62 patients.

PARTICIPANTS/MATERIALS, SETTING, METHODS: The study group consisted of 57 Japanese and five Vietnamese patients with non-syndromic hypospadias. Systematic mutation screening was performed for 25 known causative/candidate/susceptibility genes using a next-generation sequencer. Functional consequences of nucleotide alterations were assessed by *in silico* assays. The frequencies of polymorphisms in the patient group were compared with those in the male general population. CNVs were analyzed by array-based comparative genomic hybridization and characterized by fluorescence *in situ* hybridization.

MAIN RESULTS AND THE ROLE OF CHANCE: Seven of 62 patients with anterior or posterior hypospadias carried putative pathogenic mutations, such as hemizygous mutations in *AR*, a heterozygous mutation in *BNC2*, and homozygous mutations in *SRD5A2* and *HSD3B2*. Two of the seven patients had mutations in multiple genes. We did not find any rare polymorphisms that were abundant specifically in the patient group. One patient carried mosaic dicentric Y chromosome.

LIMITATIONS, REASONS FOR CAUTION: The patient group consisted solely of Japanese and Vietnamese individuals and clinical and hormonal information of the patients remained rather fragmentary. In addition, mutation analysis focused on protein-altering substitutions.

WIDER IMPLICATIONS OF THE FINDINGS: Our data provide evidence that pathogenic mutations can underlie both mild and severe hypospadias and that *HSD3B2* mutations cause non-syndromic hypospadias as a sole clinical manifestation. Most importantly, this is the first report documenting possible oligogenicity of non-syndromic hypospadias.

STUDY FUNDING/COMPETING INTERESTS: This study was funded by the Grant-in-Aid from the Ministry of Education, Culture, Sports, Science and Technology; by the Grant-in-Aid from the Japan Society for the Promotion of Science; by the Grants from the Ministry of Health, Labour and Welfare, from the National Center for Child Health and Development and from the Takeda Foundation. The authors have no competing interests to disclose.

TRIAL REGISTRATION NUMBER: Not applicable.

Key words: copy-number / hypospadias / mutation / polymorphism / susceptibility

Introduction

Hypospadias is a relatively common form of 46,XY disorders of sex development (DSD) observed in ~4–40 per 10 000 live births (Kurahashi *et al.*, 2004; Nassar *et al.*, 2007; Blaschko *et al.*, 2012). Hypospadias occurs either as an isolated anomaly or as a component of congenital malformation syndromes (Wu *et al.*, 2002; Kurahashi *et al.*, 2004). Although non-syndromic hypospadias is a multifactorial disorder induced by both genetic and environmental factors, this condition can also take place as a result of single gene mutations (Kurahashi *et al.*, 2004; Wang *et al.*, 2004; Chen *et al.*, 2007; Köhler *et al.*, 2009). Previous studies revealed familial aggregation of non-syndromic hypospadias (Schnack *et al.*, 2008; van Rooij et al., 2013). In most cases, familial hypospadias is equally transmitted from the paternal and maternal sides of the family and shows similar recurrence risks between the brothers and sons of patients, indicating a significant role of single gene mutations in the development of the disease (Schnack *et al.*, 2008).

In 2012, van der Zanden *et al.* (2012) reviewed 162 prior studies and listed 15 causative genes and three candidate genes for this condition. They also introduced 49 polymorphisms in 13 genes associated with disease risk, together with one susceptibility gene *CYP1A1* whose risk allele is yet to be determined. To date, however, there is no single report of systematic mutation analysis of the causative/candidate/susceptible genes. Likewise, while a small number of submicroscopic copy-number variations (CNVs) have been identified in patients with non-syndromic hypospadias (Tannour-Louet *et al.*, 2010), genome-wide copy-number analysis has been performed only in exceptional cases. Thus, the contribution of single gene mutations and submicroscopic CNVs to the etiology of non-syndromic hypospadias remains unknown.

The aim of this study was to clarify the frequency and type of genetic defects in patients with non-syndromic hypospadias. This study consisted of systematic mutation screening using next-generation sequencing (NGS) technology and cytogenetic analyses using comparative genomic hybridization (CGH) and fluorescence *in situ* hybridization (FISH).

Materials and Methods

Patients

A total of 57 Japanese and 5 Vietnamese patients with hypospadias participated in the study (Table I). All patients were referred to our clinics because of hypospadias. Patients with additional clinical features except for cryptorchidism and micropenis and those with cytogenetically detectable chromosomal abnormalities were excluded from this study. The 62 patients had no family history of 46,XY DSD. One of the 62 patients (case 18) was born to consanguineous parents. Hospital records of genital features at birth were obtained for 49 patients. Eleven patients manifested relatively mild hypospadias with the urethral opening at the anterior portion of the penis, while 14 and 24 patients presented with moderate (middle) and severe (posterior) hypospadias, respectively. Cryptorchidism and micropenis were observed in 5 and 11 patients, respectively.

Ethical approval

This study was approved by the Institutional Review Board Committee at the National Center for Child Health and Development and performed after obtaining written informed consent from the parents of patients.

Identification of nucleotide substitutions

Sequence analysis was carried out for 25 known causative/candidate/susceptible genes for non-syndromic hypospadias, i.e. *AR*, *ATF3*, *BMP4*, *BMP7*, *BNC2*, *CTGF*, *CYP1A1*, *CYR61*, *DGKK*, *EGF*, *ESR1*, *ESR2*, *FGF8*, *FGFR2*, *GSTM1*, *GSTT1*, *HOXA4*, *HOXB6*, *HSD3B2*, *HSD17B3*, *MAMLD1*, *MID1*, *NR5A1* (alias *SF1*), *SRD5A2*, and *WT1* (van der Zanden *et al.*, 2012). The coding regions of these genes were amplified from genomic DNA using the Haloplex Target Enrichment System (Design ID 02185-1348467147) (Agilent Technologies, Palo Alto, CA, USA), and were sequenced as 150 bp paired-end reads on a MiSeq sequencer (Illumina, San Diego, CA, USA). The average read depth of each amplicon was 115.0. Subsequently, nucleotide alterations in the samples were called by the Surecall system (Agilent Technologies) and SAMtools 0.1.17 software (http://samtools.sourceforge.net, 12 January 2015, date last accessed) (Li *et al.*, 2009). In the present study, we focused on non-synonymous substitutions in the coding regions and nucleotide changes at splice sites. Substitutions detected by NGS were confirmed by Sanger direct sequencing. The primers utilized in the present study are available upon request.

Characterization of nucleotide substitutions

Functional consequences of nucleotide alterations were predicted by *in silico* analyses. Single nucleotide polymorphisms (SNPs) with allele frequencies of >1.0% in the general population (dbSNP, http://www.ncbi.nlm.nih.gov/, 12 January 2015, date last accessed), except for those that have been reported as risk alleles (van der Zanden *et al.*, 2012), were excluded from further analyses. The effects of missense substitutions on protein function were predicted using Polyphen2 (http://genetics.bwh.harvard.edu/pph2/, 12 January 2015, date last accessed) (Adzhubei *et al.*, 2010), and those of intronic substitutions on splicing were assessed using Genome Project

Table I Nucleotide alterations identified in the present study.

Case[a]	Ethnic origin	Putative pathogenic mutation	Putative risk variant	Probable benign change	Copy-number alteration	Position of urethral opening[b]	Cryptorchidism	Micropenis
1	J	***AR* (p.S176R)**				Anterior	No	No
2	J	***AR* (p.A403V)**				No data	No data	No data
3	J	***AR* (p.R841S)**	*HSD17B3* (p.G289S)			Posterior	No	Yes
4	J	***AR* (delins[c])** *HOXB6* (p.S2N)	***MAMLD1* (p.N662S)**			No data	No data	No data
5	J	*BNC2* (p.M801R)				Posterior	No	No
6	V	***SRD5A2* (p.R227Q)[d]**	*HSD17B3* (p.G289S)			Posterior	No	Yes
7	V	***HSD3B2* (p.A10T)**	*SRD5A2* (p.R227Q)[d]			Posterior	Yes (right)	Yes
8	J		*HSD17B3* (p.G289S)	*CYP1A1* (p.T173R)	Y chromosome[e]	Posterior	No	No
9	J		***MAMLD1* (p.N662S)**			Anterior	No	No
10	J		*CYP1A1* (p.Q75P)			Middle	No data	No data
11	J		*CYP1A1* (p.A62P)			Middle	No	No
12	J		*BMP7* (p.T170M)			Middle	No	No
13	V		*HSD17B3* (p.G289S)			No data	No	No
14	J		*HSD17B3* (p.G289S)			Posterior	No	No
15	J		***HSD17B3* (p.G289S)**			Posterior	Yes	No
16	J		*HSD17B3* (p.G289S)			Posterior	No	No
17	J		*HSD17B3* (p.G289S)			Posterior	Yes (right)	Yes
18	J		*HSD17B3* (p.G289S)			Posterior	No	No
19	J		*HSD17B3* (p.G289S)			Middle	Yes (right)	Yes
20	J		*HSD17B3* (p.G289S)			Middle	No data	No data
21	J		***HSD17B3* (p.G289S)**			Middle	No	Yes
22	J		*HSD17B3* (p.G289S)			Anterior	No	No
23	J		***HSD17B3* (p.G289S)**			No data	No data	No data
24	J		*HSD17B3* (p.G289S)			No data	No data	No data
25	J		*HSD17B3* (p.G289S)			No data	No data	No data
26	J		*HSD17B3* (p.G289S) ***MAMLD1* (p.N662S)**			Middle	No	No
27	J		*HSD17B3* (p.G289S)	*BNC2* (p.M539V)		No data	No data	No data
28	J		*HSD17B3* (p.G289S)	*BNC2* (p.P614S)		No data	No data	No data
29	J		***MAMLD1* (p.N662S)**	*EGF* (p.S16R)		Posterior	No	No
30	J		*HSD17B3* (p.G289S)	*FGFR2* (p.M97V)		Anterior	No data	No data
31	J		*HSD17B3* (p.G289S)	*EGF* (p.S16R)		Middle	No	No
32	J		***MAMLD1* (p.N662S)**	*HSD3B2* (p.S284I) *EGF* (p.S16R)		Posterior	No	No

Continued

Table I *Continued*

Case[a]	Ethnic origin	Putative pathogenic mutation	Putative risk variant	Probable benign change	Copy-number alteration	Position of urethral opening[b]	Cryptorchidism	Micropenis
33	J		*HSD17B3* (p.G289S)	*HSD3B2* (p.R362W)		Anterior	No data	No data
34	J			*NR5A1* (g.IVS2-5G>A)		Posterior	No data	No data
35	J			*HOXB6* (p.P40S)		Posterior	No	Yes
36	J			***MAMLD1* (p.N675K)**		Posterior	No data	No data
37	J			*ESR2* (p.G67S)		Posterior	No	No
38	J			*EGF* (p.S16R) *BNC2* (p.I974V)		Middle	No data	No data

J, Japanese; V, Vietnamese.
Homozygous or hemizygous mutations/variations are boldfaced, and heterozygous substitutions are lightfaced.
[a]Cases 39–62 carried no nucleotide alterations in the target genes.
[b]Detailed clinical information was obtained only from 49 of the 62 patients.
[c]c.1995delTGAAGGCTATGAATGTCinsCAGAA; p.666delEGYECQinsRK.
[d]Homozygosity and heterozygosity of this mutation were described as a pathogenic defect and a disease-susceptible alteration, respectively.
[e]Copy-number gain of the region from Ypter to Yq11.223 and copy-number loss of the remaining Y chromosomal region.

Data (http://www.fruitfly.org/seq_tools/splice.html, 12 January 2015, date last accessed) (Reese *et al.*, 1997). Nucleotide deletions and insertions in the coding regions were assessed as 'probably damaging'.

Nucleotide alterations were classified into the following three groups: (i) putative pathogenic mutations: mutations that have been associated with 46,XY DSD or hitherto unreported nucleotide changes in causative genes that were assessed as 'probably damaging' or 'possibly damaging' by *in silico* analyses; (ii) putative risk variants: previously reported risk SNPs or novel substitutions in susceptibility genes, or rare SNPs in causative genes that were assessed as 'probably damaging' or 'possibly damaging'; and (iii) probable benign changes: nucleotide substitutions in causative/susceptible/candidate genes that were assessed as 'benign'. To determine the possible association between the SNPs (putative risk variants and probable benign changes) and disease risk, we compared allele frequencies in the patient group with those in the male general population. In the SNP analysis, we focused on Japanese patients, for whom the allele frequencies in the general population were available in the public database (dbSNP, http://www.ncbi.nlm.nih.gov/, 12 January 2015, date last accessed).

Statistical analysis

The statistical significance of the comparison of allele frequency in the patient group and the general population was evaluated using χ^2 and Fisher's exact probability tests.

Copy-number analyses

CNVs in the genome were screened by CGH using a catalog human array (8 × 60 k format, catalog number G4450A, Agilent Technologies), according to the manufacturers' instructions. In this study, we focused on copy-number alterations affecting genomic intervals larger than 1.5 Mb, which have a higher probability of being associated with disease phenotypes (Cooper *et al.*, 2011). We referred to the Database of Genomic Variants (http://projects.tcag.ca/variation/, 12 January 2015, date last accessed) to exclude known benign variants. Genomic structures of CNVs were characterized by FISH analysis.

Results

Identification and characterization of nucleotide substitutions

Eight putative pathogenic mutations were identified in seven patients (Table I and Fig. 1). The eight mutations consisted of three hemizygous missense mutations and one hemizygous deletion/insertion in *AR*, one heterozygous missense mutation in *HOXB6*, one heterozygous missense mutation in *BNC2*, and apparent homozygous mutations in *SRD5A2* and *HSD3B2*. Of these, the *AR* mutation in case 3 and the *SRD5A2* mutation in case 6 were previously identified in patients with 46,XY DSD (Melo *et al.*, 2003 in which the p.R841S mutation in *AR* was described as p.R840S; Sasaki *et al.*, 2003; van der Zanden *et al.*, 2012), while the other mutations were first identified in the present study.

Putative risk variants were identified in 30 patients (Table I and Supplementary Table SI). These variants included three known risk alleles for hypospadias and/or micropenis: rs2066476 in *HSD17B3*, rs2073043 in *MAMLD1* and rs9332964 in *SRD5A2* (Sasaki *et al.*, 2003; Fukami *et al.*, 2008; Sata *et al.*, 2010; Kalfa *et al.*, 2011; van der Zanden *et al.*, 2012). The SNPs in *HSD17B3* and *MAMLD1* were identified in the Japanese patient group and the male general population at similar frequencies. We also identified a rare SNP in the causative gene *CYP1A1* which was shared by the Japanese patients and the male

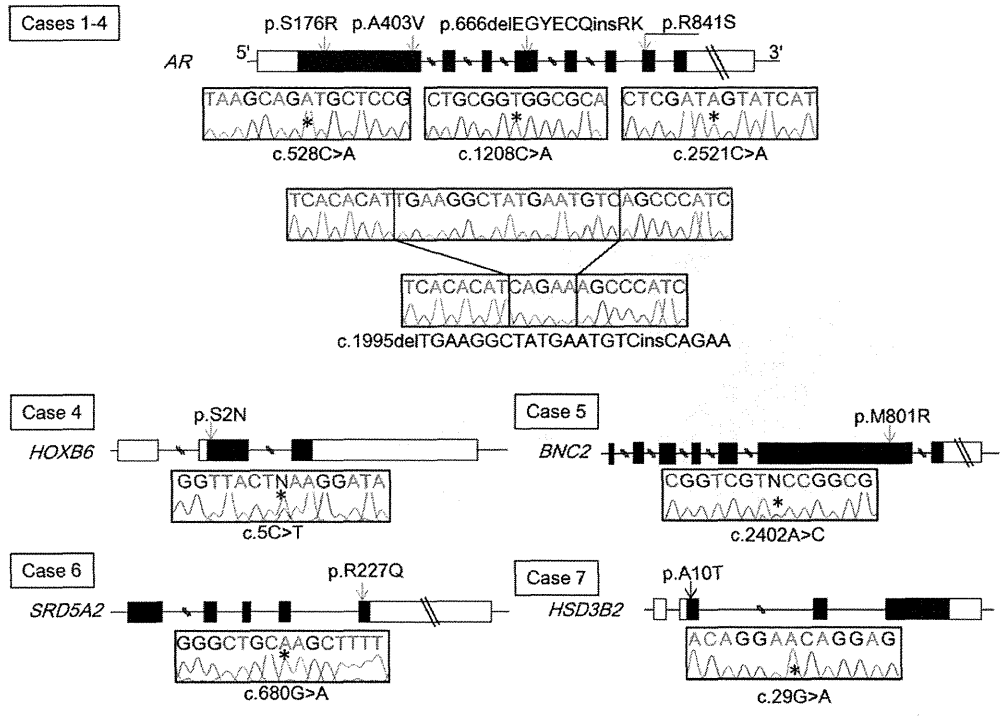

Figure 1 Putative pathogenic mutations identified in the present study. Genomic positions and chromatograms of the nucleotide substitutions are shown. Asterisks indicate the mutated nucleotides.

general population at a similar frequency, together with a SNP in *BMP4* whose frequency in the general population is unknown.

Probable benign changes were found in 13 patients (Table I and Supplementary Table SI). These substitutions included a rare SNP in *EGF* which was identified in the patient group and in the general population at similar frequency. We also detected SNPs in *ESR2* and *BNC2* that had unknown frequencies in the general population, together with a novel substitution in intron 2 of *NR5A1* (g.IVS2-5G>A) that was predicted to not affect splicing.

Copy-number analyses

One of the 62 patients (case 8) carried CNVs on the Y chromosome (Fig. 2A). These alterations consisted of copy-number gain of a ~23 Mb region from Ypter to Yq11.223 and copy-number loss of the remaining Y chromosomal region. The log2 signal ratios of most probes corresponding to the amplified and deleted regions were lower than +1.0 and higher than −2.0 respectively, indicating mosaicism of these CNVs. FISH analysis using a *SRY*-containing probe showed that case 8 had mosaic dicentric Y (Fig. 2B). CGH analysis for case 6 with an apparently homozygous *SRD5A2* mutation and case 7 with an apparently homozygous *HSD3B2* mutation excluded compound heterozygosity for a mutation and deletion (data not shown).

Clinical findings of patients with putative pathogenic defects

Putative pathogenic defects were associated with both anterior and posterior hypospadias (Table II). Endocrine evaluation of cases 1–8 remained fragmentary; blood hormone levels in cases 3 and 7 were within the normal range (Table II).

Discussion

Systematic mutation screening identified putative pathogenic mutations in 7 of 62 patients with non-syndromic hypospadias. These results, in conjunction with previous studies showing that ~30% of cases with severe hypospadias are ascribable to specific defects such as mutations in *AR* or *SRD5A2* (Albers *et al.*, 1997; Boehmer *et al.*, 2001), demonstrate the significant role of mutations in known causative genes in the etiology of non-syndromic hypospadias. Furthermore, our results support the previously proposed notion that genetic defects in *AR* account for a substantial percentage of cases with various types of 46,XY DSD (Albers *et al.*, 1997; Boehmer *et al.*, 2001; Audi *et al.*, 2010) and that mutations in *HSD3B2* can lead to non-syndromic hypospadias as a sole clinical manifestation, although *HSD3B2* plays an essential role in adrenal function (Boehmer *et al.*, 2001; Codner *et al.*, 2004; Audi *et al.*, 2010). Case 3 carried the p.R841S mutation in *AR*, which have been identified in patients with ambiguous genitalia (Melo *et al.*, 2003), suggesting the phenotypic diversity of missense mutations in *AR*. Notably, two of our patients had putative pathogenic mutations in multiple genes. Case 4 carried a hemizygous in-frame deletion/insertion in *AR* and a heterozygous missense substitution in *HOXB6*. Likewise, case 7 with a homozygous missense mutation in *HSD3B2* had an additional heterozygous missense mutation in *SRD5A2* that retains 3% of enzymatic activity (Makridakis *et al.*, 2000; Sasaki *et al.*, 2003). These data imply for the

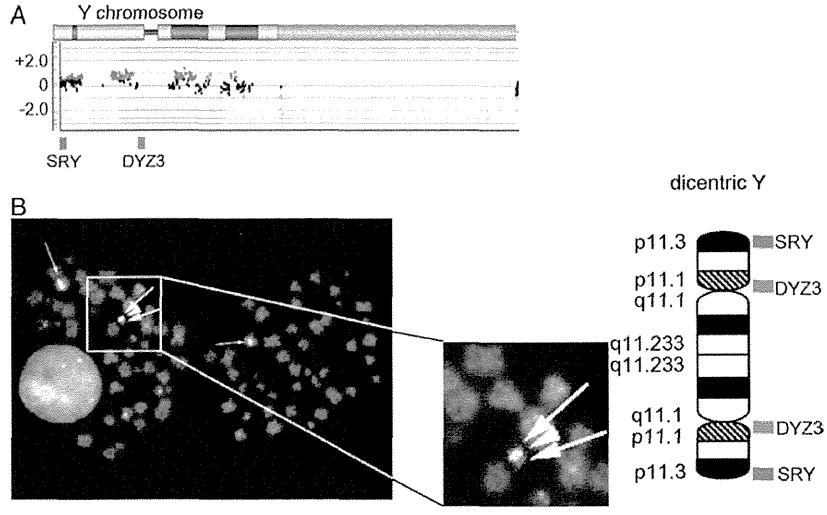

Figure 2 Copy-number alterations identified in case 8. Results of array-based comparative genomic hybridization (CGH) (**A**) and fluorescence *in situ* hybridization (FISH) analysis and schematic representation of the dicentric Y chromosome (**B**) are shown. The black, red and green dots in CGH denote signals indicative of the normal, increased (> +0.4) and decreased (< −0.8) copy-numbers, respectively. The arrowhead and thick arrows in FISH indicate a signal of DYZ3 (Y centromeric probe) and signals of *SRY*-containing probe (Yp11.3), respectively. The thin arrows in the left panel indicate signals of X centromeric probe.

Table II Molecular and clinical findings of patients with putative pathogenic abnormalities.

	Case 1	Case 2	Case 3	Case 4	Case 5	Case 6	Case 7	Case 8
Affected gene/region	*AR*	*AR*	*AR*	*AR/HOXB6*	*BNC2*	*SRD5A2*	*HSD3B2*	Y chromosome[a]
Ethnic origin	Japanese	Japanese	Japanese	Japanese	Japanese	Vietnamese	Vietnamese	Japanese
Family history of DSD	No	No data	No	No data	No	No	No	No
Clinical features								
Hypospadias[b]	Anterior	No data	Posterior	No data	Posterior	Posterior	Posterior	Posterior
Cryptorchidism	No	No data	No	No data	No	No	Yes (right)	No
Micropenis	No	No data	Yes	No data	No	Yes	Yes	No
Other features	No	No data	No	No data	No	No	No	Borderline MR
Endocrine findings								
Age at examination	No data	No data	15 months	No data	No data	No data	3.5 years	No data
LH (IU/l)[c]	No data	No data	<0.2 (<0.2–0.3)	No data	No data	No data	No data	No data
FSH (IU/l)[c]	No data	No data	<1.0 (<1.0–1.5)	No data	No data	No data	No data	No data
Testosterone (nmol/l)[c]	No data	No data	0.17 (0.10–0.45)	No data	No data	No data	0.16 (0.10–0.45)	No data

DSD, disorders of sex development; MR, mental retardation; LH, luteinizing hormone; FSH, follicle stimulating hormone.
[a]Copy-number alterations on Y chromosome.
[b]Position of urethral opening.
[c]Hormone values in parentheses indicate the reference ranges of age- and sex-matched control individuals.

first time that non-syndromic hypospadias results from digenic mutations. On the other hand, we did not observe the accumulation of rare SNPs in the patient group. Our data suggest that previously reported susceptibility SNPs play no or only minor roles in the development of non-syndromic hypospadias in the Japanese population. However, we cannot exclude the possibility that oligogenicity of these SNPs increases the risk of the disease, because a small number of our patients carried these SNPs as biallelic or digenic substitutions. Considering the small number of participants of this study, further investigations are necessary to clarify the possible association between rare SNPs and the disease phenotype.

Genome-wide copy-number analysis identified cryptic CNVs only in one patient. Case 8 carried a copy-number gain of a ~23 Mb region

on Yp and Yq and copy-number loss of the remaining Y chromosomal region. FISH analysis revealed that case 8 had mosaic dicentric Y, which has been described in multiple patients with hypospadias (Drummond-Borg *et al.*, 1988; Kojima *et al.*, 2001). It has been proposed that dicentric Y results in hypospadias by mosaic loss of the rearranged Y chromosome or by aberrant expression of Y chromosomal genes (Drummond-Borg *et al.*, 1988; Kojima *et al.*, 2001). The lack of pathogenic CNVs in the remaining 61 cases suggests the rarity of cryptic CNVs as genetic causes of non-syndromic hypospadias.

In this study, putative pathogenic defects were identified predominantly in patients with severe (posterior) hypospadias, while an *AR* mutation was detected in case 1, who manifested mild (anterior) hypospadias without micropenis or cryptorchidism. In this regard, previous studies have shown that syndromic hypospadias often arises from known gene mutations or chromosomal rearrangements (van der Zanden *et al.*, 2012). These data imply that monogenic mutations can underlie various types of hypospadias, although they are more strongly associated with severe or syndromic hypospadias than with mild non-syndromic hypospadias. Since identification of pathogenic defects can help to predict disease outcomes and improves the accuracy of genetic counseling, genetic analyses should be considered in patients with hypospadias of various clinical severities.

It should be pointed out that the present study has some limitations. First, the patient group consisted of only Japanese and Vietnamese individuals. Since the prevalence of hypospadias varies among countries (Nassar *et al.*, 2007; Serrano *et al.*, 2013), there may be ethnicity-specific causes of hypospadias. For example, mutations in *ATF3*, which account for ~10% of cases in the USA (Kalfa *et al.*, 2008), were absent from our cohort. In contrast, the p.A10T mutation in *HSD3B2* and the p.R227Q mutation in *SRD5A2* were detected exclusively in Vietnamese patients in homozygous state. Thus, our results are not simply applicable to other ethnic groups. Second, the frequency of monogenic defects may be underestimated in this study, because we focused on protein-altering mutations in 25 genes. Mutations/variations in regulatory regions, defects in unexamined genes and epigenetic abnormalities may be hidden in our mutation-negative patients. Lastly, clinical information of our patients remained fragmentary. Although previous studies have revealed that several factors such as low birthweight, placental insufficiency and maternal hypertension are associated with the risk of hypospadias (Stoll *et al.*, 1990; Weidner *et al.*, 1999; Fredell *et al.*, 2002; Brouwers *et al.*, 2010), the contributions of such factors to the disease phenotype of our patients are yet to be studied. Moreover, since endocrine data were unavailable for most of our mutation-positive cases, further studies are needed to elucidate the hormonal characteristics of each monogenic disorder.

Conclusion

The present study indicates that mutations in known causative genes and submicroscopic CNVs account for > 10% of cases with non-syndromic hypospadias. Pathogenic defects appear to underlie both severe and mild hypospadias. On the other hand, previously reported risk SNPs are unlikely to play a major role in the development of the disease; further studies are required to validate this observation. Most importantly, this is the first report documenting the possible oligogenicity of non-syndromic hypospadias.

Supplementary data

Supplementary data are available at http://humrep.oxfordjournals.org/.

Authors' roles

M.K., K.No., T.O., and M.F. designed the study. M.K., E.S., V.C.D., Y.H., T.M., K.Mu., K.U., N.I., K.Nag., Y.O., T.H., K.Y., M.I, Y.K.-F., K.Nak., K.Hay., K.Hat., Y.M., K.Mo., and T.O. contributed to the acquisition of data. M.K. and M.F. analyzed data and wrote the paper. All authors were involved in revising the paper and approved the final version of the manuscript for submission.

Funding

This study was funded by the Grant-in-Aid from the Ministry of Education, Culture, Sports, Science and Technology; by the Grant-in-Aid from the Japan Society for the Promotion of Science; by the Grants from the Ministry of Health, Labour and Welfare, from the National Center for Child Health and Development and from the Takeda Foundation.

Conflict of interest

The authors declare that there is no conflict of interest.

References

Adzhubei IA, Schmidt S, Peshkin L, Ramensky VE, Gerasimova A, Bork P, Kondrashov AS, Sunyaev SR. A method and server for predicting damaging missense mutations. *Nat Methods* 2010;**7**:248–249.

Albers N, Ulrichs C, Glüer S, Hiort O, Sinnecker GH, Mildenberger H, Brodehl J. Etiologic classification of severe hypospadias: implications for prognosis and management. *J Pediatr* 1997;**131**:386–392.

Audi L, Fernández-Cancio M, Carrascosa A, Andaluz P, Torán N, Piró C, Vilaró E, Vicens-Calvet E, Gussinyé M, Albisu MA *et al.* Novel (60%) and recurrent (40%) androgen receptor gene mutations in a series of 59 patients with a 46,XY disorder of sex development. *J Clin Endocrinol Metab* 2010;**95**:1876–1888.

Blaschko SD, Cunha GR, Baskin LS. Molecular mechanisms of external genitalia development. *Differentiation* 2012;**84**:261–268.

Boehmer AL, Nijman RJ, Lammers BA, de Coninck SJ, Van Hemel JO, Themmen AP, Mureau MA, de Jong FH, Brinkmann AO, Niermeijer MF *et al.* Etiological studies of severe or familial hypospadias. *J Urol* 2001; **165**:1246–1254.

Brouwers MM, van der Zanden LF, de Gier RP, Barten EJ, Zielhuis GA, Feitz WF, Roeleveld N. Hypospadias: risk factor patterns and different phenotypes. *BJU Int* 2010;**105**:254–262.

Chen T, Li Q, Xu J, Ding K, Wang Y, Wang W, Li S, Shen Y. Mutation screening of BMP4, BMP7, HOXA4 and HOXB6 genes in Chinese patients with hypospadias. *Eur J Hum Genet* 2007;**15**:23–28.

Codner E, Okuma C, Iñiguez G, Boric MA, Avila A, Johnson MC, Cassorla FG. Molecular study of the 3 beta-hydroxysteroid dehydrogenase gene type II in patients with hypospadias. *J Clin Endocrinol Metab* 2004;**89**:957–964.

Cooper GM, Coe BP, Girirajan S, Rosenfeld JA, Vu TH, Baker C, Williams C, Stalker H, Hamid R, Hannig V *et al.* A copy number variation morbidity map of developmental delay. *Nat Genet* 2011;**43**:838–846.

Drummond-Borg M, Pagon RA, Bradley CM, Nordlund J, Salk D. Nonfluorescent dicentric Y in males with hypospadias. *J Pediatr* 1988; **113**:469–473.

Fredell L, Kockum I, Hansson E, Holmner S, Lundquist L, Lackgren G, Pedersen J, Stenberg A, Westbacke G, Nordenskjöld A. Heredity of hypospadias and the significance of low birth weight. *J Urol* 2002;**167**:1423–1427.

Fukami M, Wada Y, Okada M, Kato F, Katsumata N, Baba T, Morohashi K, Laporte J, Kitagawa M, Ogata T. Mastermind-like domain-containing 1 (MAMLD1 or CXorf6) transactivates the Hes3 promoter, augments testosterone production, and contains the SF1 target sequence. *J Biol Chem* 2008;**283**:5525–5532.

Kalfa N, Liu B, Klein O, Wang MH, Cao M, Baskin LS. Genomic variants of ATF3 in patients with hypospadias. *J Urol* 2008;**180**:2183–2188.

Kalfa N, Cassorla F, Audran F, Oulad Abdennabi I, Philibert P, Béroud C, Guys JM, Reynaud R, Alessandrini P, Wagner K *et al.* Polymorphisms of MAMLD1 gene in hypospadias. *J Pediatr Urol* 2011;**7**:585–591.

Köhler B, Lin L, Mazen I, Cetindag C, Biebermann H, Akkurt I, Rossi R, Hiort O, Gruters A, Achermann JC. The spectrum of phenotypes associated with mutations in steroidogenic factor 1 (SF-1, NR5A1, Ad4BP) includes severe penoscrotal hypospadias in 46,XY males without adrenal insufficiency. *Eur J Endocrinol* 2009;**161**:237–242.

Kojima Y, Hayashi Y, Yanai Y, Tozawa K, Sasaki S, Kohri K. Molecular analysis of hypospadias in a boy with dicentric Y chromosome. *J Urol* 2001; **165**:1244–1245.

Kurahashi N, Murakumo M, Kakizaki H, Nonomura K, Koyanagi T, Kasai S, Sata F, Kishi R. The estimated prevalence of hypospadias in Hokkaido, Japan. *J Epidemiol* 2004;**14**:73–77.

Li H, Handsaker B, Wysoker A, Fennell T, Ruan J, Homer N, Marth G, Abecasis G, Durbin R. The Sequence Alignment/Map format and SAMtools. *Bioinformatics* 2009;**25**:2078–2079.

Makridakis NM, di Salle E, Reichardt JK. Biochemical and pharmacogenetic dissection of human steroid 5 alpha-reductase type II. *Pharmacogenetics* 2000;**10**:407–413.

Melo KF, Mendonca BB, Billerbeck AE, Costa EM, Inácio M, Silva FA, Leal AM, Latronico AC, Arnhold IJ. Clinical, hormonal, behavioral, and genetic characteristics of androgen insensitivity syndrome in a Brazilian cohort: five novel mutations in the androgen receptor gene. *J Clin Endocrinol Metab* 2003;**88**:3241–3250.

Nassar N, Bower C, Barker A. Increasing prevalence of hypospadias in Western Australia, 1980–2000. *Arch Dis Child* 2007;**92**:580–584.

Reese MG, Eeckman FH, Kulp D, Haussler D. Improved splice site detection in Genie. *J Comput Biol* 1997;**4**:311–323.

Sasaki G, Ogata T, Ishii T, Kosaki K, Sato S, Homma K, Takahashi T, Hasegawa T, Matsuo N. Micropenis and the 5alpha-reductase-2 (SRD5A2) gene: mutation and V89L polymorphism analysis in 81 Japanese patients. *J Clin Endocrinol Metab* 2003;**88**:3431–3436.

Sata F, Kurahashi N, Ban S, Moriya K, Tanaka KD, Ishizuka M, Nakao H, Yahata Y, Imai H, Kakizaki H *et al.* Genetic polymorphisms of 17 beta-hydroxysteroid dehydrogenase 3 and the risk of hypospadias. *J Sex Med* 2010;**7**:2729–2738.

Schnack TH, Zdravkovic S, Myrup C, Westergaard T, Christensen K, Wohlfahrt J, Melbye M. Familial aggregation of hypospadias: a cohort study. *Am J Epidemiol* 2008;**167**:251–256.

Serrano T, Chevrier C, Multigner L, Cordier S, Jégou B. International geographic correlation study of the prevalence of disorders of male reproductive health. *Hum Reprod* 2013;**28**:1974–1986.

Stoll C, Alembik Y, Roth MP, Dott B. Genetic and environmental factors in hypospadias. *J Med Genet* 1990;**27**:559–563.

Tannour-Louet M, Han S, Corbett ST, Louet JF, Yatsenko S, Meyers L, Shaw CA, Kang SH, Cheung SW, Lamb DJ. Identification of *de novo* copy number variants associated with human disorders of sexual development. *PLoS One* 2010;**5**:e15392.

van der Zanden LF, van Rooij IA, Feitz WF, Franke B, Knoers NV, Roeleveld N. Aetiology of hypospadias: a systematic review of genes and environment. *Hum Reprod Update* 2012;**18**:260–283.

van Rooij IA, van der Zanden LF, Brouwers MM, Knoers NV, Feitz WF, Roeleveld N. Risk factors for different phenotypes of hypospadias: results from a Dutch case-control study. *BJU Int* 2013;**112**:121–128.

Wang Y, Li Q, Xu J, Liu Q, Wang W, Lin Y, Ma F, Chen T, Li S, Shen Y. Mutation analysis of five candidate genes in Chinese patients with hypospadias. *Eur J Hum Genet* 2004;**12**:706–712.

Weidner IS, Møller H, Jensen TK, Skakkebaek NE. Risk factors for cryptorchidism and hypospadias. *J Urol* 1999;**161**:1606–1609.

Wu WH, Chuang JH, Ting YC, Lee SY, Hsieh CS. Developmental anomalies and disabilities associated with hypospadias. *J Urol* 2002; **168**:229–232.

Tissue and Cell 46 (2014) 470–476

Contents lists available at ScienceDirect

Tissue and Cell

journal homepage: www.elsevier.com/locate/tice

Short communication

Arm-specific telomere dynamics of each individual chromosome in induced pluripotent stem cells revealed by quantitative fluorescence *in situ* hybridization

Masanori Terai[a,b,*], Naotaka Izumiyama-Shimomura[a], Junko Aida[a], Naoshi Ishikawa[a], Mie Kuroiwa[c], Tomio Arai[d], Masashi Toyoda[e,f], Ken-ichi Nakamura[a], Kaiyo Takubo[a,**]

[a] Research Team for Geriatric Pathology, Tokyo Metropolitan Institute of Gerontology, Tokyo 173-0015, Japan
[b] Department of Judotherapy, Faculty of Health Sciences, Tokyo Ariake University of Medical and Health Sciences, Tokyo 135-0063, Japan
[c] Department of Analytical Chemistry, Yokohama College of Pharmacy, Yokohama 245-0066, Japan
[d] Department of Pathology, Tokyo Metropolitan Geriatric Hospital, Tokyo 173-0015, Japan
[e] Research Team for Vascular Medicine, Tokyo Metropolitan Institute of Gerontology, Tokyo 173-0015, Japan
[f] Department of Reproductive Biology, National Research Institute for Child Health and Development, Tokyo 157-8535, Japan

ARTICLE INFO

Article history:
Received 10 May 2014
Received in revised form 2 August 2014
Accepted 16 August 2014
Available online 27 August 2014

Keywords:
Telomere
iPSC
Q-FISH
TFU
Chromosome arm

ABSTRACT

We have reported that telomere fluorescence units (TFUs) of established induced pluripotent stem cells (iPSCs) derived from human amnion (hAM933) and fetal lung fibroblasts (MRC-5) were significantly longer than those of the parental cells, and that the telomere extension rates varied quite significantly among clones without chromosomal instability, although the telomeres of other iPSCs derived from MRC-5 became shorter as the number of passages increased along with chromosomal abnormalities from an early stage. In the present study we attempted to clarify telomere dynamics in each individual chromosomal arm of parental cells and their derived clonal human iPSCs at different numbers of passages using quantitative fluorescence in situ hybridization (Q-FISH). Although no specific arm of any particular chromosome appeared to be consistently shorter or longer than most of the other chromosomes in any of the cell strains, telomere elongation in each chromosome of an iPSC appeared to be random and stochastic. However, in terms of the whole genome of any specific cell, the telomeres showed overall elongation associated with iPSC generation. We have thus demonstrated the specific telomere dynamics of each individual chromosomal arm in iPSCs derived from parental cells, and in the parental cells themselves, using Q-FISH.

1. Introduction

Normal human cells exhibit a limited capacity for proliferation in culture (Hayflick, 1965). This phenomenon is considered to be attributable to reduction of telomere length as an indicator of the number of divisions a cell has undergone. Telomeres protect chromosomes against degeneration, reconstruction, fusion and loss, as well as contributing to pairing of homologous chromosomes (Blackburn, 1991). Telomeres are repetitive G-rich DNA sequences found at the ends of linear eukaryotic chromosomes and appear to play a key role in preventing genomic instability (Blackburn, 2001). The end-to-end chromosome fusions observed in some tumors could play a role in genetic instability associated with tumorigenesis, and may be the result of telomere loss (Blackburn, 1991). The human telomere is a simple repeating sequence of six bases, TTAGGG, located at the ends of chromosomes (Moyzis et al., 1988). Telomere lengths of cultured fibroblasts (Takubo et al., 2010) and human tissues (Aida et al., 2008) show marked heterogeneity among individual telomeres, and in terms of mean or median values in individual cells. Heterogeneity of telomere length and telomerase expression has also been reported previously among induced pluripotent stem cells (iPSCs) and cultured fibroblasts (Wang et al., 2012). In the present study we attempted to clarify telomere dynamics in each individual chromosomal arm of both parental cells and their derived clonal human iPSCs after different numbers of passages using quantitative fluorescence in situ hybridization (Q-FISH).

* Corresponding author at: Department of Judotherapy, Faculty of Health Sciences, Tokyo Ariake University of Medical and Health Sciences, 2-9-1 Ariake, Koto-ku, Tokyo 135-0063, Japan. Tel.: +81 3 6703 7061; fax: +81 3 6703 7061.
** Corresponding author. Fax: +81 3 3579 4776.
E-mail addresses: terai@tau.ac.jp, teramasa@agate.plala.or.jp (M. Terai), Takubo@tmig.or.jp (K. Takubo).

http://dx.doi.org/10.1016/j.tice.2014.08.005
0040-8166/

Q-FISH and image analyses were performed as described previously. The Q-FISH method we have developed and employed is highly accurate and reproducible, having already been used in a number of published studies (Izumiyama-Shimomura et al., 2014; Nakamura et al., 2014; Poon and Lansdorp, 2001a, 2001b; Takubo et al., 2010; Terai et al., 2013).

Previously we have measured individual telomere lengths of chromosomal arms in human fibroblast strains using Q-FISH to clarify the morphologic signs of chromosomal instability (Takubo et al., 2010). We have demonstrated a linear correlation between telomere fluorescence units (TFUs) estimated by Q-FISH and telomere length measured by Southern blotting (Takubo et al., 2010). We have reported that TFUs of iPSCs derived from human amnion (hAM933) and fetal lung fibroblasts (MRC-5) were significantly longer than those of the parental cells, and that the telomere extension rates varied quite significantly among clones without chromosomal instability, although the telomeres of other iPSCs derived from MRC-5 became shorter as the number of passages increased, along with chromosomal abnormalities from an early stage (Terai et al., 2013). Here, using Q-FISH, we investigated the specific telomere dynamics of each individual chromosomal arm in iPSCs cloned from parental cells, and also the parental cells from which they were derived, after different numbers of passages in culture.

2. Materials and methods

2.1. Ethics statement

Human amnion cells were collected by scraping tissue from surgical specimens, with signed informed consent from the donors concerned, and under ethical approval from the Institutional Review Board of the National Institute for Child Health and Development, Japan. The surgical specimens were irreversibly de-identified. All experiments involving the handling of human cells and tissues were performed in line with the tenets of the Declaration of Helsinki.

2.2. Human cell culture

Human amniotic membrane (hAM)-derived cells were independently established in our laboratory (Cui et al., 2007, 2011; Fukawatase et al., 2014; Makino et al., 2009; Nagata et al., 2009; Nishino et al., 2010, 2011). hAM-derived cells and MRC-5 cells were maintained in Dulbecco's modified Eagle medium (DMEM) supplemented with 10% fetal bovine serum and penicillin–streptomycin. Human iPSCs were generated in our laboratory using the procedures described by Yamanaka and colleagues (Cui et al., 2007, 2011; Fukawatase et al., 2014; Makino et al., 2009; Nagata et al., 2009; Nishino et al., 2010, 2011; Takahashi and Yamanaka, 2006; Takahashi et al., 2007). The iPSCs were established from hAM-derived cells and MRC-5, and designated hAM933 iPSCs and MRC-5 iPSCs, respectively. Briefly, to produce VSV-G (vesicular stomatitis virus G glycoprotein) retroviruses, 293FT cells (Invitrogen) were plated at 2×10^6 cells per 10-cm culture dish in DMEM supplemented with 10% FBS, and incubated overnight. On the following day, the cells were co-transfected with pMXs-OCT4, SOX2, KLF4 or c-MYC, pCL-GagPol, and pHCMV-VSV-G vectors using the TransIT-293 reagent (Mirus Bio LLC, Madison, WI, USA). The virus-containing supernatants were collected 48 h after incubation. The supernatants were filtered through a 0.45-mm pore size filter, centrifuged, and then resuspended in DMEM supplemented with 4 mg/ml polybrene (Nakarai Tesque, Kyoto, Japan). The parental cells were seeded at 1×10^5 cells per well in 6-well Plates 24 h before infection. A 1:1:1:1 mixture of OCT4, SOX2, KLF4 and c-MYC viruses was then added to the parental cells (Cui et al., 2007, 2011; Fukawatase et al., 2014; Makino et al., 2009; Nagata et al., 2009; Nishino et al., 2010, 2011; Takahashi and Yamanaka, 2006; Takahashi et al., 2007). In a separate experiment, infection with the retrovirus carrying the EGFP gene was performed to estimate the infection efficiency. One half of the medium was changed every day, and colonies were picked up at around day 28. They were maintained on irradiated mouse embryonic fibroblasts (MEFs) in iPSellon medium (Cardio Incorporated, Kobe, Japan) supplemented with 10 ng/ml recombinant human basic fibroblast growth factor (bFGF, Wako Pure Chemical Industries, Ltd., Osaka, Japan). We used iPSCs that had been chosen randomly from stable lines in our laboratory.

We measured telomere lengths of each individual chromosomal arm in the parental cells (hAM933 and MRC-5), two iPSC lines (hAM933 iPSCs-2, hAM933 iPSCs-3) derived from different colonies originating from hAM933, and two iPSC lines (MRC-5 iPSCs-16 and MRC-5 iPSCs-40) cloned from the same iPSCs (MRC-5 iPSCs) at different numbers of passages (MRC-5 iPSCs-16; passages 22 and 59; MRC-5 iPSCs-40; passages 21 and 62).

We checked cell contamination by short tandem repeat (STR) genotyping of the parental cells (hAM933 and MRC-5), two iPSC lines (hAM933 iPSCs-2, hAM933 iPSCs-3) derived from different colonies originating from hAM933, and two iPSC lines (MRC-5 iPSCs-16 and MRC-5 iPSCs-40) cloned from the same iPSCs (MRC-5 iPSCs) after different numbers of passages (data not shown) (Cui et al., 2007, 2011; Fukawatase et al., 2014; Makino et al., 2009; Nagata et al., 2009; Nishino et al., 2010, 2011; Takahashi and Yamanaka, 2006; Takahashi et al., 2007). Genomic DNA was isolated from samples of the cultured cells using DNeasy columns (Qiagen). This DNA was used as a template for STR analysis employing the PowerPlex 16 System (Promega) and ABI PRISM instrumentation. Numbers shown denote the bp lengths of the 15 autosomal fragments. The analysis was carried out at BEX Co., Ltd.

2.3. Measurement of telomere lengths of individual arms in metaphase spreads using Q-FISH and image analysis

For karyotype analysis and quantitative analysis of telomeres, metaphase chromosomes were fixed and then hybridized using the peptide nucleic acid-FISH preparation method described previously (Poon and Lansdorp, 2001a; 2001b).

A Cy3-labeled $(CCCTAA)_3$ peptide nucleic acid probe (telo C) (Fasmac, Atsugi, Catalog No. F1002, Japan) was used to label the telomeres, and a FITC-labeled CTTCGTTGGAAACGGGGT peptide nucleic acid probe (CENP1; a non-specific centromere probe; Fasmac, custom made, Japan) was used for labeling the centromere. The chromosome preparations were counterstained with 4′,6-diamidino-2-phenylindole (DAPI, Molecular Probes, Eugene, OR, USA).

Analysis of fluorescence images was performed as described previously (Takubo et al., 2010). Digital images were recorded with a CCD camera, AxioCam MRm (Zeiss, Oberkochen, Germany), mounted on an Axio Imager M1 (Zeiss) epifluorescence microscope equipped with a triple band-pass filter for Cy3/FITC/DAPI (61010 Chroma Technology, Corp., Rockingham, VT, USA) and a 63× oil objective lens (Zeiss EC Plan-NEOFLUAR 63×/1.25 ∞/0.17). Microscope control and image acquisition were performed with the ISIS system (MetaSystems, GmbH, Altlussheim, Germany).

A calibration system was used to ensure reliable quantitative estimation of telomere length in the various samples. To correct for daily variations in lamp intensity and alignment, images of fluorescent beads (orange beads, size 0.2 μm, Molecular Probes Inc.) were imaged just prior to acquisition of images from the samples. The fluorescence intensities of the beads and the telomeres

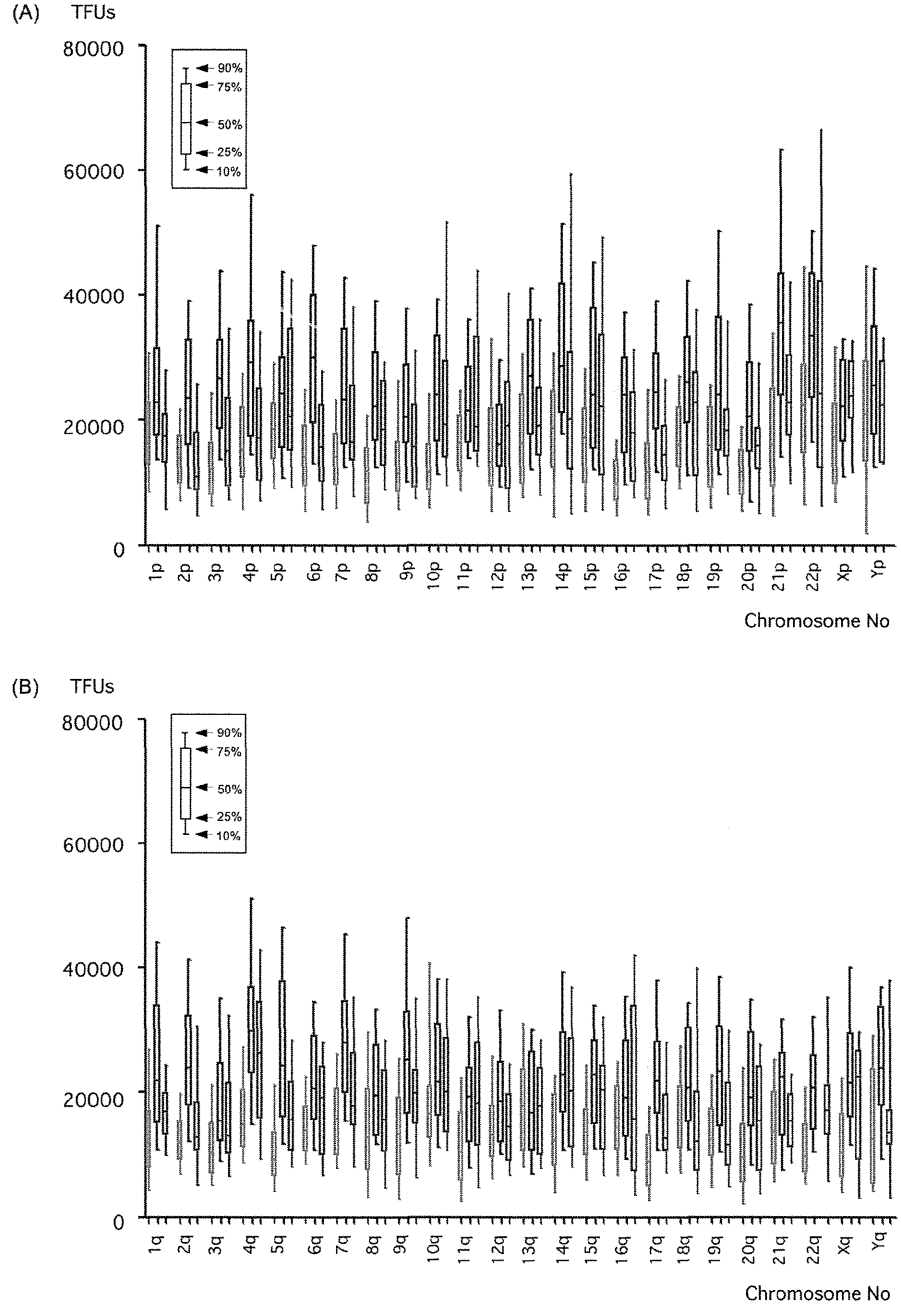

Fig. 1. Mean values of the median arm-specific telomere lengths (TFUs) of each individual chromosomal arm for 20 metaphase spreads in hAM933 parental cells, and two iPSCs (hAM933 iPSCs-2, hAM933 iPSCs-3) derived from different colonies originating from hAM933. The telomere fluorescence units (TFUs) of the p-arms (A) and q-arms (B) of each chromosome in the spread were measured individually. Mean values of the median telomere lengths (TFUs) of 20 metaphase spreads in the parental cells (hAM933, passage 3), hAM933 iPSCs-2 (passage 25) and hAM933 iPSCs-3 (passage 27) are shown as box plots (hAM933, passage 3; red box plots, hAM933 iPSCs-2, passage 25; blue box plots, and hAM933 iPSCs-3, passage 27; green box plots) for all analyzed data. Raw data for the subjects overall are listed in Supplementary Information (A). (For interpretation of the references to colour in this figure legend, the reader is referred to the web version of this article.)

were analyzed using the TFLTelo-V2 software package (Terry Fox Laboratory, BC Cancer Research Centre, Canada).

Using the ISIS karyotyping system, we analyzed the karyotypes of 20 metaphase spreads at early passage (hAM933, passage 3, MRC-5, and MRC-5 iPSCs-16 and 40, passages 22 and passages 21, respectively) and late passage (hAM933 iPSCs-2, passage 25, hAM933 iPSCs-3, passage 27, MRC-5 iPSCs-16, passage 59 and MRC-5 iPSCs-40, passage 62). We then measured the telomere fluorescence intensities of the p- and q-arms of all the chromosomes in the spread individually.

The median TFU value was defined as a representative value for a metaphase spread (184 telomeres), and the mean value of the median values of the p- and q-arms from the karyotyped metaphase spreads was calculated to determine whether there was any chromosome-specific extension or shortening of telomeres related to specific p- or q-arms. Differences in mean values were assessed for significance by Student's t-test and correlations by Fisher's test, using the methods reported previously (Izumiyama-Shimomura et al., 2014; Nakamura et al., 2014; Takubo et al., 2010; Terai et al., 2013).

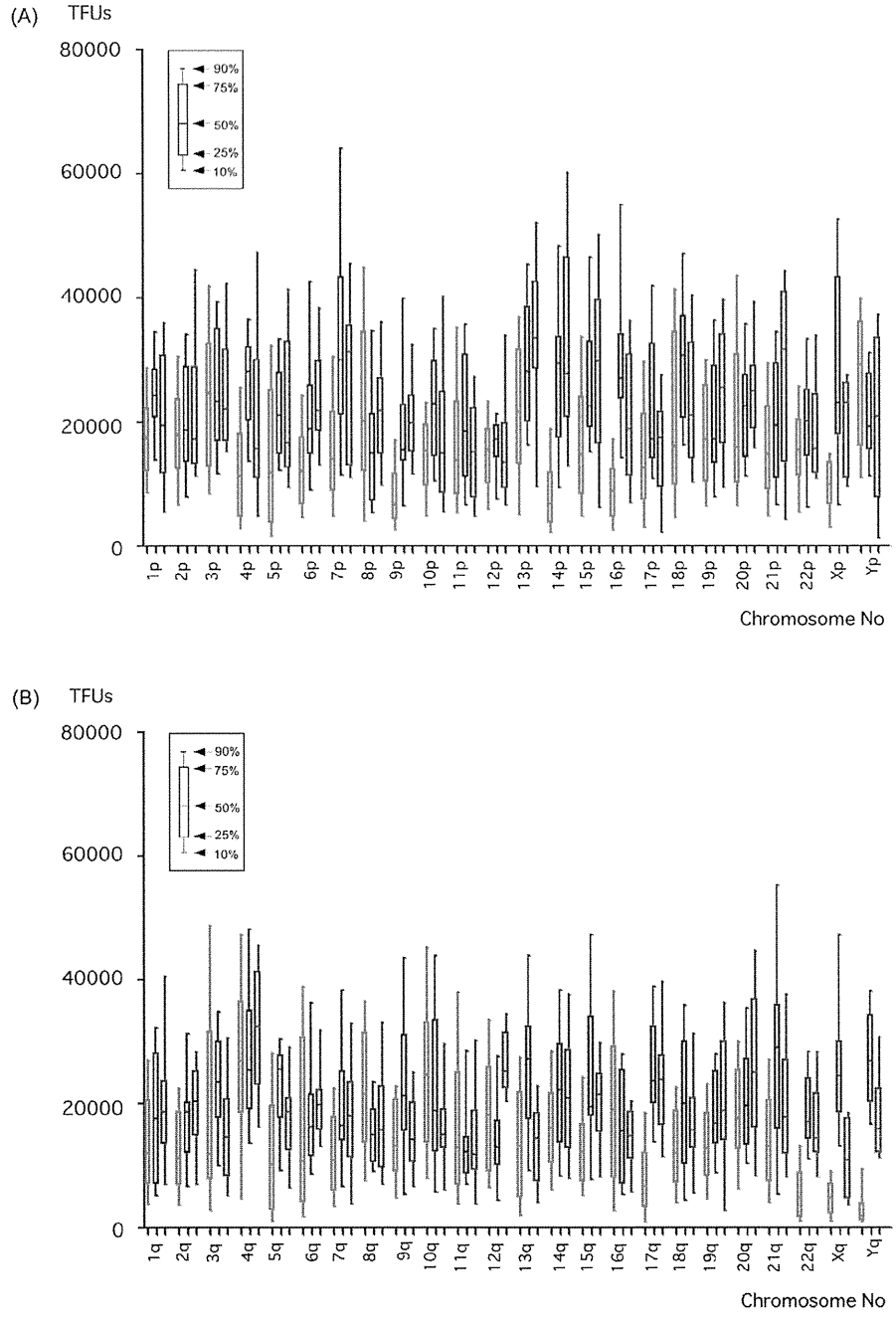

Fig. 2. Mean values of the median arm-specific telomere lengths (TFUs) of each individual chromosomal arm for 20 metaphase spreads in MRC-5 parental cells, and MRC-5 iPSCs-16 cloned from MRC-5 iPSCs after different numbers of passages (passages 22 and 59). The telomere fluorescence units (TFUs) of the p-arms (A) and q-arms (B) of each chromosome in the spread were measured individually. Mean values of the median telomere lengths (TFUs) of 20 metaphase spreads in MRC-5 and MRC-5 iPSCs-16 (passages 22 and 59) are shown as box plots (MRC-5; red box plots, MRC-5 iPSCs-16, passages 22; blue box plots, and MRC-5 iPSCs-16, passages 59; green box plots) for all analyzed data. Raw data for the subjects overall are listed in Supplementary Information (B). (For interpretation of the references to colour in this figure legend, the reader is referred to the web version of this article.)

3. Results

Arm-specific telomere lengths (TFUs) of each individual chromosomal arm in the parental cells (hAM933), and two iPSC lines (hAM933 iPSCs-2, hAM933 iPSCs-3) derived from different colonies originating from hAM933, are summarized in Fig. 1.

Chromosomal arms of hAM933 iPSCs-2 showed significant extension in the order 1p, 1q, 2p, 2q, 3p, 3q, 4p, 4q, 5q, 6p, 6q, 7p, 7q, 8p, 9p, 9q, 10p, 11p, 11q, 13p, 14p, 14q, 15p, 15q, 16p, 17p, 17q, 18p, 18q, 19p, 19q, 20p, 20q, 21p, 21q, 22p, 22q, Xq and Yq, in comparison with the parental hAM933 cells. Chromosomal arms of hAM933 iPSCs-3 showed significant extension in the order 4q, 8p, 10p, 11p, 11q, 16p, 17q and 22q, in comparison with the parental hAM933 cells. Chromosomal arms of hAM933 iPSCs-2 showed significant differences in the order 2p, 2q, 3p, 6p, 17p and 17q, in comparison with hAM933 iPSCs-3. Raw data for the subjects overall are listed in Supplementary Information (A).

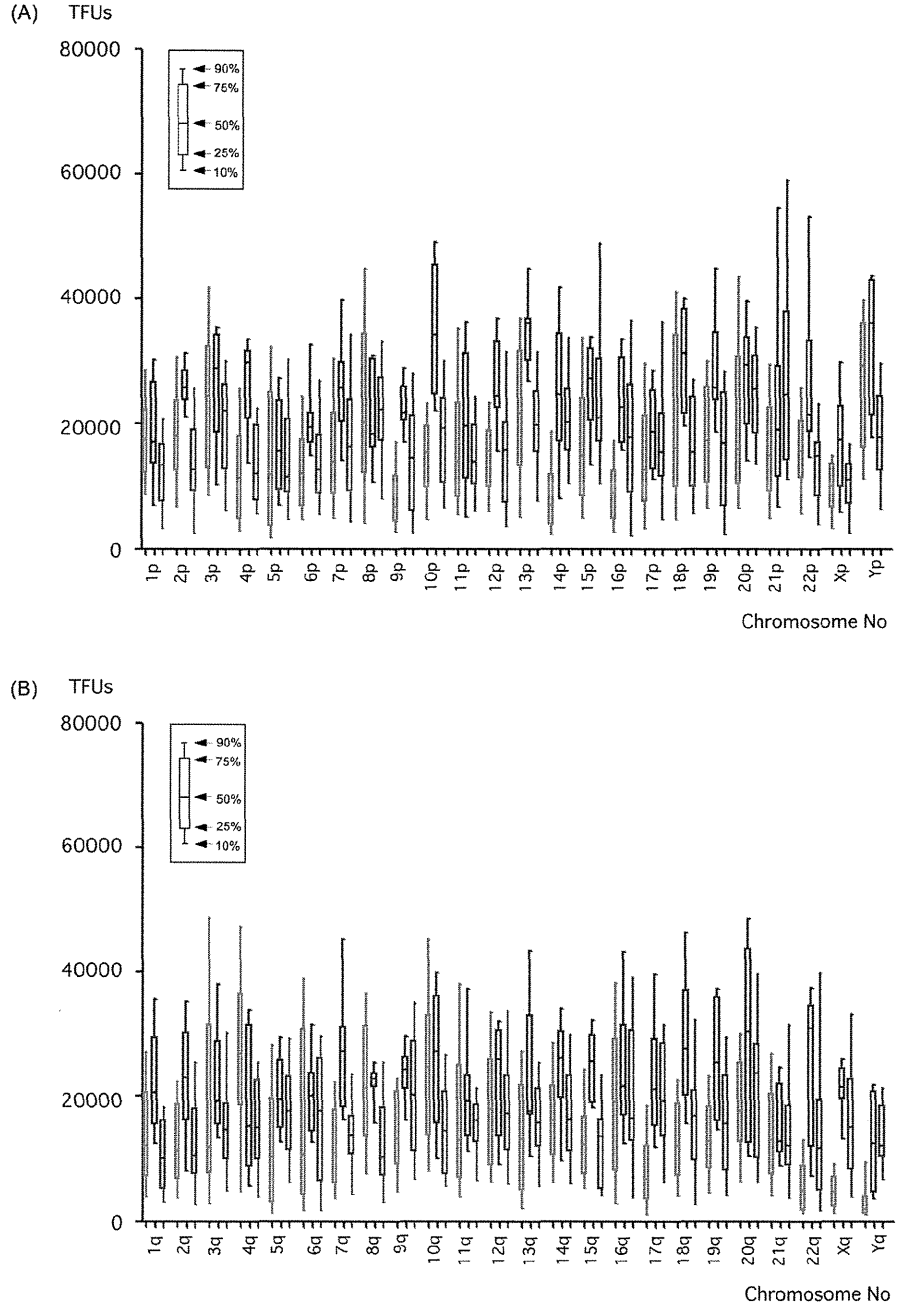

Fig. 3. Mean values of the median arm-specific telomere lengths (TFUs) of each individual chromosomal arm for 20 metaphase spreads in MRC-5 parental cells, and MRC-5 iPSCs-40 cloned from MRC-5 iPSCs after different numbers of passages (passages 21 and 62). The telomere fluorescence units (TFUs) of the p-arms (A) and q-arms (B) of each chromosome in the spread were measured individually. Mean values of the median telomere lengths (TFUs) of 20 metaphase spreads in MRC-5 and MRC-5 iPSCs-40 (passages 21 and 62) are shown as box plots (MRC-5; red box plots, MRC-5 iPSCs-40, passages 21; blue box plots, and MRC-5 iPSCs-40, passages 62; green box plots) for all analyzed data. Raw data for the subjects overall are listed in Supplementary Information (C). (For interpretation of the references to colour in this figure legend, the reader is referred to the web version of this article.)

Arm-specific telomere lengths (TFUs) of each individual chromosomal arm in the parental cells (MRC-5), and in MRC-5 iPSCs-16 and MRC-5 iPSCs-40 cloned from the same iPSCs (MRC-5 iPSCs) at different numbers of passages (MRC-5 iPSCs-16; passages 22 and 59; MRC-5 iPSCs-40; passages 21 and 62) are summarized in Fig. 2 (MRC-5 iPSCs-16) and Fig. 3 (MRC-5 iPSCs-40), respectively.

Chromosomal arms of MRC-5 iPSCs-16 (P22) showed significant extension in the order 4p, 7p, 9p, 9q, 13q, 14p, 15q, 16p, 17q, 21q, 22q, Xp, Xq and Yq, in comparison with the parental MRC-5 cells. Chromosomal arms of MRC-5 iPSCs-16 (P59) showed significant extension in the order 6p, 7p, 9p, 14p, 16p, 17q, 22q, Xp and Yq, in comparison with the parental MRC-5 cells. The arms of chromosome 12q in MRC-5 iPSCs-16 (P22) showed a significant difference from those in MRC-5 iPSCs-16 (P59). Raw data for the subjects overall are listed in Supplementary Information (B).

Chromosomal arms of MRC-5 iPSCs-40 (P21) showed significant extension in the order 7q, 9p, 10p, 12p, 14p, 15q, 16p, 17q, 18q, 19q, 22q, Xq and Yq, in comparison with the parental MRC-5 cells. Chromosomal arms of MRC-5 iPSCs-40 (P62) showed significant extension in the order 14p, 16p, 17q, 21p, 22q, Xq and Yq, and a

significant reduction in the order 4q and 8q, in comparison with the parental MRC-5 cells. Chromosomal arms of MRC-5 iPSCs-40 (P62) showed significant reduction in the order 1q, 2p, 4p, 7q, 10p, 13p, 15q and 18p, in comparison with MRC-5 iPSCs-40 (P21) as the number of passages increased (21 and 62). Raw data for the subjects overall are listed in Supplementary Information (C).

No specific arm of any particular chromosome appeared to be consistently shorter or longer than most of the other chromosomes in any of the cell strains, except for the 16p, 17q and 22q arms. Although telomere elongation did not appear to be random and stochastic in these three arms, telomere elongation in each chromosome of an iPSC appeared to be almost random and stochastic.

4. Discussion

The establishment of iPSCs appears to be associated with telomere elongation and activation of telomerase (Takahashi and Yamanaka, 2006; Takahashi et al., 2007). Human iPSCs are derived from a patient's own cells, and thus present no immunological or ethical problems. It is believed that it will be possible to obtain iPSCs in sufficient numbers for treatment and reconstruction of extensive defects. Development of human iPSCs is at an advanced stage, and their clinical application is expected.

We have already reported that TFUs of iPSCs established from hAM933 were significantly longer than those of the parental cells, and that the telomere extension rates varied quite significantly among clones without any apparent chromosomal instability (Terai et al., 2013). Although no specific arm of any particular chromosome appeared to be consistently shorter or longer than most of the other chromosomes in any of the cell strains among the clones, telomere elongation in each chromosome of an iPSC was random and stochastic. However, in terms of the whole genome of any specific cell, the telomeres showed overall elongation associated with iPSC generation. This suggests that there is TFU heterogeneity among the various chromosomes in iPSC clones.

We have already reported that TFUs of iPSCs established from MRC-5 cells were significantly longer than those of the parental cells, and that the telomere extension rates varied quite significantly without any apparent chromosomal instability, although the telomeres of other iPSCs derived from MRC-5 became shorter as the number of passages increased, along with chromosomal abnormalities from an early stage (Terai et al., 2013). Significant extension of chromosome 12q in MRC-5 iPSCs-16 was observed from an early stage as the number of passages increased, in the absence of any chromosomal abnormalities. However, eight chromosomal arms of MRC-5 iPSCs-40 showed a significant reduction in length as the number of passages increased and also the minimum TFU of MRC-5 iPSC-40 (passage 62, TFU; 371) was smaller than that of MRC-5 (TFU; 380). These results indicate that MRC-5 iPSC-40 with telomere shortening would be more susceptible to karyotype abnormality (Terai et al., 2013).iPSCs are heterogeneous, and individual iPSCs also show a wide range of telomerase expression and telomere length (Wang et al., 2012). Telomeres become elongated upon establishment of iPSCs, which also acquire telomerase activity and epigenetic changes. Establishment of iPSCs requires a process of epigenetic reprogramming (Reik, 2007). The culture conditions used for iPSCs would influence random methylation and convergence, and telomere activation might be influenced by epigenetic regions of hTERT transcription (Reik, 2007). This process would be dependent on the epigenetic information in each individual iPSC. Epigenetic information is present in the form of DNA methylation, and culture of iPSCs under various conditions can result in stochastic de novo methylation (Nishino et al., 2010, 2011).

Here, using Q-FISH, we were able to demonstrate the arm-specific telomere dynamics of each of the individual chromosomal arms in cloned iPSCs derived from parental cells, and in the parental cells themselves, after different numbers of passages in culture. If iPSCs are applied for cell therapies in the future, reprogramming techniques will be critical to control the expression of specific genes in individual cells, and standardization of the basic biology of iPSCs will also be needed to ensure their practical application. Measurement of telomeres in individual chromosomes of a cell would also be needed for guaranteeing the quality of iPSCs. Further studies will be necessary to clarify the telomere dynamics responsible for controlling the genetic expression of individual iPSCs.

Funding

This work was supported by JSPS KAKENHI: 21390109 (K.T.), 16590300 (K.N.) and 25670182 (M.T), and a research grant from the Ministry of Health, Labor and Welfare Sciences (MHLW) (M.T.).

Competing financial interests statement

The authors have no conflicts of interest to declare in relation to this study.

Appendix A. Supplementary data

Supplementary data associated with this article can be found, in the online version, at http://dx.doi.org/10.1016/j.tice.2014.08.005.

References

Aida, J., Izumiyama-Shimomura, N., Nakamura, K., Ishikawa, N., Poon, S.S., Kammori, M., Sawabe, M., Arai, T., Matsuura, M., Fujiwara, M., Kishimoto, H., Takubo, K., 2008. Basal cells have longest telomeres measured by tissue Q-FISH method in lingual epithelium. Exp. Gerontol. 43, 833–839.

Blackburn, E.H., 1991. Structure and function of telomeres. Nature 350, 569–573.

Blackburn, E.H., 2001. Switching and signaling at the telomere. Cell 106, 661–673.

Cui, C.H., Miyoshi, S., Tsuji, H., Makino, H., Kanzaki, S., Kami, D., Terai, M., Suzuki, H., Umezawa, A., 2011. Dystrophin conferral using human endothelium expressing HLA-E in the non-immunosuppressive murine model of Duchenne muscular dystrophy. Hum. Mol. Genet. 20, 235–244.

Cui, C.H., Uyama, T., Miyado, K., Terai, M., Kyo, S., Kiyono, T., Umezawa, A., 2007. Menstrual blood-derived cells confer human dystrophin expression in the murine model of Duchenne muscular dystrophy via cell fusion and myogenic transdifferentiation. Mol. Biol. Cell 18, 1586–1594.

Hayflick, L., 1965. The limited in vitro lifetime of human diploid cell strains. Exp. Cell Res. 37, 614–636.

Fukawatase, Y., Toyoda, M., Okamura, K., Nakamura, K., Nakabayashi, K., Takada, S., Yamazaki-Inoue, M., Masuda, A., Nasu, M., Hata, K., Hanaoka, K., Higuchi, A., Takubo, K., Umezawa, A., 2014. Ataxia telangiectasia derived iPS cells show preserved X-ray sensitivity and decreased chromosomal instability. Sci. Rep. 4, 5421.

Izumiyama-Shimomura, N., Nakamura, K., Aida, J., Ishikawa, N., Kuroiwa, M., Hiraishi, N., Fujiwara, M., Ishikawa, Y., Inoshita, N., Yonese, J., Matsuura, M., Poon, S.S., Arai, T., Takubo, K., 2014. Short telomeres and chromosome instability prior to histologic malignant progression and cytogenetic aneuploidy in papillary urothelial neoplasms. Urol. Oncol. 32, 135–145.

Makino, H., Toyoda, M., Matsumoto, K., Saito, H., Nishino, K., Fukawatase, Y., Machida, M., Akutsu, H., Uyama, T., Miyagawa, Y., Okita, H., Kiyokawa, N., Fujino, T., Ishikawa, Y., Nakamura, T., Umezawa, A., 2009. Mesenchymal to embryonic incomplete transition of human cells by chimeric OCT4/3 (POU5F1) with physiological co-activator EWS. Exp. Cell Res. 315, 2727–2740.

Moyzis, R.K., Buckingham, J.M., Cram, L.S., Dani, M., Deaven, L.L., Jones, M.D., Meyne, J., Ratliff, R.L., Wu, J.R., 1988. A highly conserved repetitive DNA sequence $(TTAGGG)_n$, present at the telomeres of human chromosomes. Proc. Natl. Acad. Sci. U.S.A. 85, 6622–6626.

Nagata, S., Toyoda, M., Yamaguchi, S., Hirano, K., Makino, H., Nishino, K., Miyagawa, Y., Okita, H., Kiyokawa, N., Nakagawa, M., Yamanaka, S., Akutsu, H., Umezawa, A., Tada, T., 2009. Efficient reprogramming of human and mouse primary extra-embryonic cells to pluripotent stem cells. Genes Cells 14, 1395–1404.

Nakamura, K., Ishikawa, N., Izumiyama, N., Aida, J., Kuroiwa, M., Hiraishi, N., Fujiwara, M., Nakao, A., Kawakami, T., Poon, S.S., Matsuura, M., Sawabe, M., Arai, T., Takubo, K., 2014. Telomere lengths at birth in trisomy 18 and 21 measured by Q-FISH. Gene 533, 199–207.

Nishino, K., Toyoda, M., Yamazaki-Inoue, M., Fukawatase, Y., Chikazawa, E., Sakaguchi, H., Akutsu, H., Umezawa, A., 2011. DNA methylation dynamics in human induced pluripotent stem cells over time. PLoS Genet. 7, e1002085.

Nishino, K., Toyoda, M., Yamazaki-Inoue, M., Makino, H., Fukawatase, Y., Chikazawa, E., Takahashi, Y., Miyagawa, Y., Okita, H., Kiyokawa, N., Akutsu, H., Umezawa,

A., 2010. Defining hypo-methylated regions of stem cell-specific promoters in human iPS cells derived from extra-embryonic amnions and lung fibroblasts. PLoS ONE 5, e13017.

Poon, S.S., Lansdorp, P.M., 2001a. Quantitative fluorescence in situ hybridization (Q-FISH). Curr. Protoc. Cell Biol., 4 (Chapter 18; Unit 18).

Poon, S.S., Lansdorp, P.M., 2001b. Measurements of telomere length on individual chromosomes by image cytometry. Methods Cell Biol. 64, 69–96.

Reik, W., 2007. Stability and flexibility of epigenetic gene regulation in mammalian development. Nature 447, 425–432.

Takahashi, K., Tanabe, K., Ohnuki, M., Narita, M., Ichisaka, T., Tomoda, K., Yamanaka, S., 2007. Induction of pluripotent stem cells from adult human fibroblasts by defined factors. Cell 131, 861–872.

Takahashi, K., Yamanaka, S., 2006. Induction of pluripotent stem cells from mouse embryonic and adult fibroblast cultures by defined factors. Cell 126, 663–676.

Takubo, K., Aida, J., Izumiyama, N., Ishikawa, N., Fujiwara, M., Poon, S.S., Kondo, H., Kammori, M., Matsuura, M., Sawabe, M., Arai, T., Baird, D.M., Nakamura, K., 2010. Chromosomal instability and telomere lengths of each chromosomal arm measured by Q-FISH in human fibroblast strains prior to replicative senescence. Mech. Ageing Dev. 131, 614–624.

Terai, M., Izumiyama-Shimomura, N., Aida, J., Ishikawa, N., Kuroiwa, M., Poon, S.S., Arai, T., Toyoda, M., Akutsu, H., Umezawa, A., Nakamura, K., Takubo, K., 2013. Investigation of telomere length dynamics in induced pluripotent stem cells using quantitative fluorescence in situ hybridization. Tissue Cell 45, 407–413.

Wang, F., Yin, Y., Ye, X., Liu, K., Zhu, H., Wang, L., Chiourea, M., Okuka, M., Ji, G., Dan, J., Zuo, B., Li, M., Zhang, Q., Liu, N., Chen, L., Pan, X., Gagos, S., Keefe, D.L., Liu, L., 2012. Molecular insights into the heterogeneity of telomere reprogramming in induced pluripotent stem cells. Cell Res. 22, 757–768.